Neural Modelling for Synthesis of Sector Beam and Multibeam Array Antennas

R.Ghayoula[1], N.Fadlallah[2], A.Gharsallah[3], M.Rammal[4]

ABSTRACT

A new and very speedy low-sidelobe pattern synthesis method for linear array antennas with periodic element spacing is described. This paper presents an efficient method for the pattern synthesis based on neural network modelling and Fourier transform method.

The proposed synthesis method provides important improvements in terms of performance, computational speed, elasticity, and ease of implementation in software to the methods described in literature. A number of representative examples are presented to demonstrate the various unique capabilities of the method. The results include sum and difference patterns for antenna array.

The approach combines a neural network with the hardware limitations of the array to place nulls in the directions of interference with small perturbations to the far-field pattern. Excellent nulling results are possible for most interference scenarios.

Keywords : Sector beam, Fourier method, neural network, multibeam array antennas, synthesis method.

1. INTRODUCTION

Its often necessary to design an antenna array with certain radiation characteristics. It may be necessary to have the nulls in certain direction, or it may be necessary to have the major lobe directed in a certain direction; also there may be requirements for the direction and the level of the side lobes. This is termed as beam shaping, and there are some techniques to synthesize the arrays with a given beam shape.

Fourier transforms method [1-2] can be used to determine, given a complete description of the desired pattern, the excitation distribution of a discrete source antenna system. The derived excitation yields, either precisely or approximately, the desired antenna pattern. Since physically only finite dimension apertures are feasible, the excitation distribution is limited and one can search only for approximated solutions. Every time the desired pattern contains discontinuities or its values in a given region change very rapidly, the reconstruction pattern will exhibit oscillatory overshoots which are referred to as Gibbs' phenomenon. On the other hand the radiation pattern of an array is the product of an array factor and the radiation pattern of a single antenna. As a result only in the case of isotropic antenna calculated excitation distribution yields the desired radiation pattern of the array.

The Fourier transform method is the best suited for patterns, which are analytically simple and can be integrated easily. The integration required for this method can be done numerically with a computer with height efficiency.

The inherent nonlinearities associated with antenna radiation patterns make antennas very suitable candidates

[1] Laboratoire de physique de la matière molle, Unité de recherche : Circuits et systèmes électroniques HF Faculté des Sciences de Tunis, Campus Universitaire Tunis EL-manar, 2092, Tunisie.

[2] Equipe RADICOM, Institut Universitaire de Technologie de Saida Université de Liban, P.O.Box #813 36, Liban.

for NNs [2]. Neural networks have been used successfully in:

1-Varying the usable bandwidth of microstrip patch antennas.

2- Estimating the angle of arrival of signals in a mobile communication environment.

3- Determining the excitation coefficients in phased array antennas to change the direction of the radiation beam for target.

The method described here uses NNs to predict the excitations coefficients (amplitude and phases). The NNs is trained with a set of the design parameters and their corresponding radiation patterns. Once the NNs have been trained, it can be used to predict the design parameters if a new pattern are presented to it. Actually the network can be trained to predict the complex weights (the amplitude and phase).

In this paper we propose a simple analytical method which takes into consideration the influence of the radiation pattern of a single antenna on the resultant array radiation pattern. The method was verified experimentally for the case of sector beam radiation pattern of quasi-yagi antenna arrays.

The paper is organized as follows. In section II, the problem formulation of one-dimensional array is shown with the relation of the weights, array factor and translated wavenumber with Fourier method. In section III, numerical results from various computer simulations are shown to present the overall performance of the proposed technique in section IV, the neural network based on back-propagation technique is developed and applied for synthesis of antenna array. In section V simulation and measurement result. Finally, section VI summarizes the concluding remarks of this paper.

2. Problem Formulation

The mathematical model for a linear array with isotropic antenna elements lying along the x axis with elements positioned at locations x_n, n = 0, 1, 2. . . n ,will have displacement vectors $d_n = x_n \hat{x}$ is given by:

$$AF(\theta,\varphi) = \sum_n i_n e^{jk.d_n} = \sum_n i_n e^{jk_x x_n \sin\theta\cos\varphi} \qquad (1)$$

Where we set $k_x = k\sin\theta\cos\varphi$ For equally-spaced arrays, the element locations are $x_n = nd$, where d is the distance between elements. In this case, the array factor becomes:

$$AF(\theta,\varphi) = \sum_n i_n e^{jnkd\sin\theta\cos\varphi} \qquad (2)$$

Because the angular dependence comes through the factor $k_x d = kd\sin\theta\cos\varphi$, [3] we are led to define the variable: $\psi = k_x d = kd\sin\theta\cos\varphi$ (Digital wave number) Then, the array factor may be thought of as a function of ψ Where :

$k = \frac{2\pi}{\lambda}$ wave number.

λ wavelength.

d spacing between elements.

φ angle of incidence of electromagnetic plane wave.

$i_n = |i_n| e^{j\varphi_n}$ Complex array weight at element m.

n number of elements.

$$AF(\psi) = \sum_n i_n e^{i\psi n} \qquad (4)$$

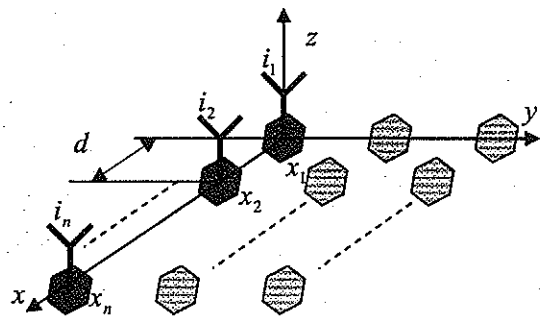

Figure 1 : Geometry Of a N-element Equally Spaced Linear Array Along X-axis. Which Has n Equally Spaced Elements Along The Axis. The Element Spacing Is Half-Wavelength.

A. Fourier Series Method

This method is practical to determine the amplitude distribution of a continuous line source, but can be adapted to determine the excitation amplitude of an antenna array. The method is based on the inverse [4, 5] discrete-space Fourier transforms of the array factor.

i) If N is odd, say $N = 2M+1$, we can define the element locations x_m symmetrically as:

$$x_m = md, \qquad m = 0,\pm1,\pm2,...,\pm M$$

The array factor can be written then as a discrete-space Fourier transform:

$$\begin{aligned} AF(\psi) &= \sum_{m=-M}^{M} i_m e^{jm\psi} \\ &= i_0 + \sum_{m=1}^{M}\left[i_m e^{jm\psi} + i_{-m} e^{-jm\psi}\right] \end{aligned} \tag{5}$$

ii) If N is even, say $N = 2M$, in order to have symmetry with respect to the origin, we must place the elements at the half-integer locations:

$$x_{\pm m} = \pm\left(md - \frac{d}{2}\right) = \pm\left(md - \frac{1}{2}\right)d, \; m = 1,2,...,M$$

The array factor will be now:

$$AF(\psi) = \sum_{m=1}^{M}\left[i_m e^{j(m-1/2)\psi} + i_{-m} e^{-j(m-1/2)\psi}\right] \tag{6}$$

In particular, if the array weights am are symmetric with respect to the origin, $i_m = i_{-m}$, as they are in most design methods, then the array factor can be simplified into the cosine forms:

$$\begin{aligned} AF(\psi) &= i_0 + 2\sum_{m=1}^{M} i_m \cos(m\psi), \quad (N = 2M+1) \\ AF(\psi) &= 2\sum_{m=1}^{M} i_m \cos((m-1/2)\psi), \quad (N = 2M) \end{aligned} \tag{7}$$

As an example of the Fourier series method, we discuss the design of an array with angular pattern confined into a desired angular sector.

First, we consider the design in ψ space of an ideal bandpass array factor centered at wavenumber ψ_0 with bandwidth of $2\psi_b$. We will see later how to map these specifications into an actual angular sector [3]. The ideal bandpass response is defined over $-\pi \le \psi \le \pi$ as follows:

$$AF_{BP}(\psi) = \begin{cases} 1, & \psi_0 - \psi_b \le \psi \le \psi_0 + \psi_b \\ 0, & otherwise \end{cases} \tag{8}$$

For the odd case, the corresponding ideal weights are inverse transform.

$$\begin{aligned} i_{BP}(m) &= \frac{1}{2\pi}\int_{-\pi}^{\pi} AF_{BP}(\psi) e^{-jm\psi} d\psi \\ &= \frac{1}{2\pi}\int_{\psi_0-\psi_b}^{\psi_0+\psi_b} 1.e^{-jm\psi} d\psi \end{aligned} \tag{9}$$

Which gives:

$$i_{BP}(m) = e^{-jm\psi_0}\frac{\sin(\psi_b m)}{\pi m}, m = 0,\pm1,\pm2,... \tag{10}$$

This problem is equivalent to designing an ideal lowpass response with cut-off frequency ψ_b and then translating it by

$$AF_{BP}(\psi) = AF_{LP}(\psi') = AF_{LP}(\psi - \psi_0)$$

where $\psi' = \psi - \psi_0$. The lowpass response is defined as:

$$AF_{LP}(\psi) = \begin{cases} 1, & -\psi_b \le \psi' \le \psi_b \\ 0, & otherwise \end{cases} \qquad (11)$$

and its ideal weights are:

$$i_{LP}(m) = \frac{1}{2\pi}\int_{-\pi}^{\pi} AF_{LP}(\psi')e^{-jm\psi'}d\psi' = \frac{1}{2\pi}\int_{-\psi_b}^{\psi_b} 1.e^{-jm\psi'}d\psi'$$

$$= \frac{\sin(\psi_b m)}{\pi m}$$

Therefore, as expected, the ideal weights for the bandpass and lowpass designs are related by a scanning phase:

$$i_{BP}(m) = e^{-jm\psi_0} i_{LP}(m) \qquad (13)$$

Therefore, the design specifications are the quantities $(\psi_p, \psi_{p'}, A)$. Alternatively, we can take them to be $(\psi_p, \Delta\psi, A)$, where $\Delta\psi = \psi_{p'} - \psi_p$ is the transition width.

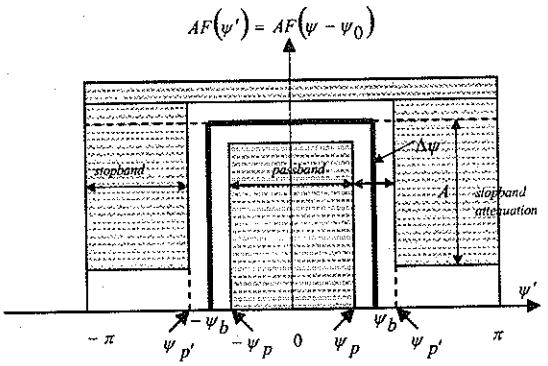

Figure 2 : Specifications Of Equivalent Lowpass Response.

The propose steps for the bandpass response using the Kaiser window are summarized below (Fig.3):

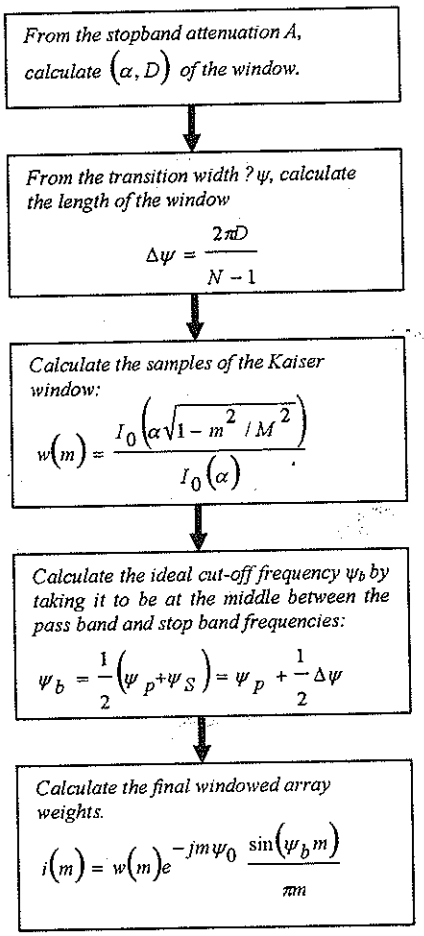

Figure 3 : The Design Steps For The Bandpass Response Using The Kaiser Window

Where

$I_0(x)$: Bessel functions of first kind and zeroth order.

D, α : Window parameters.

The propose method can be extended to the case of even $N = 2M$. The Kaiser window remains the same for $m = \pm1, \pm2, ..., \pm M$. We note the symmetry $w(-m) = w(m)$. After windowing and scanning with ψ_0, we get the final designed weights:

$$i(\pm m) = w(m)e^{\pm j(m-1/2)\psi_0}\frac{\sin(\psi_b(m-1/2))}{\pi(m-1/2)} \qquad (14)$$

$$m = 1,2,...,M$$

After that, we use the above bandpass design in ψ-space to design an array with an angular sector response in φ space. The ideal array will have a pattern that is uniformly flat over an angular sector $[\varphi_1, \varphi_2]$:

$$AF(\varphi) = \begin{cases} 1, & \varphi_1 \le \varphi \le \varphi_2 \\ 0, & otherwise \end{cases} \qquad (15)$$

C- Multibeam Arrays

An array can form multiple narrow beams towards different directions. For example, suppose it is desired to form three beams towards the steering angles φ_1, φ_2, and φ_3.

The weights for such a multibeam array can be obtained by superimposing the weights of a single broadside array, [6] say i(m), steered towards the three angles. Defining the corresponding scanning phase's $\psi_i = kd\cos\varphi_i$, i = 1, 2, 3, we have:

$$AF(m) = A_1 e^{-jm\psi_1} i(m) + A_2 e^{-jm\psi_2} i(m) + A_3 e^{-jm\psi_3} i(m) \qquad (16)$$

Where m = 0, ±1, ±2. . .±M and we assumed an odd number of array elements N = 2M + 1. The complex amplitudes A1, A2, A3 represent the relative importance of the three beams. The corresponding array factor becomes:

$$AF(\psi) = A_1 i(\psi - \psi_1) + A_2 i(\psi - \psi_2) + A_3 i(\psi - \psi_3) \qquad (17)$$

and will exhibit narrow peaks towards the three steering angles. More generally, we can form L beams towards the angles φ_i, i = 1, 2. . . L by superimposing the steered beams:

$$AF(m) = \sum_{i=1}^{L} A_i e^{-jm\psi_i} i(m), \quad m = 0,\pm1,\pm2,...,\pm M \qquad (18)$$

where $\psi_i = kd\cos\varphi_i$, i = 1, 2, . . . , L.

$$i(m) = w(m) e^{-jm\psi_0} \frac{\sin(\psi_b m)}{\pi m} \qquad (19)$$
$$m = 0,\pm1,\pm2,...,\pm M$$

For an even number of array elements, N = 2M, we replace Eq (18) with:

$$AF(\pm m) = \sum_{i=1}^{L} A_i e^{\pm j(m-1/2)\psi_i} i(\pm m), \quad m = 1,2,...,M \qquad (20)$$

Where

$$i(\pm m) = w(m) e^{\pm j(m-1/2)\psi_0} \frac{\sin(\psi_b (m-1/2))}{\pi(m-1/2)} \qquad (21)$$
$$m = 1,2,...,M$$

For either even or odd N, the corresponding array factor will be the superposition:

$$AF(\psi) = \sum_{i=1}^{L} A_i\, i(\psi - \psi_i) \qquad (22)$$

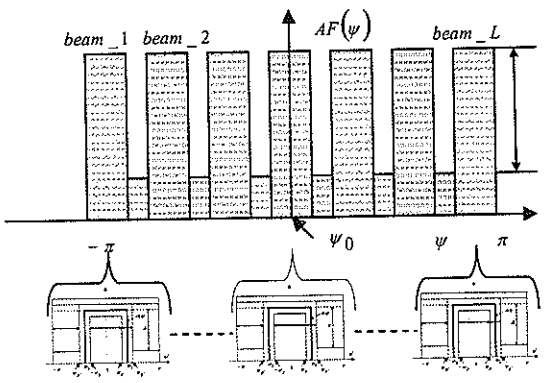

Figure 4 : Multibeam Array (Desired Radiation Pattern)

To illustrate the performance of the method described in the earlier section for steering single and multiple beams in desired direction by controlling the amplitude and phase excitation of each array element, three examples of uniform excited linear array with N = 16, one-half wavelength spaced isotropic elements were performed.

The results of steering beam in the direction of the desired signal are presented in Figs 5, 6 and 7.

In this section the Fourier transform method is applied so as to determine the excitation coefficients and the

resultant pattern for a broadside discrete element array whose array factor will closely approximate the symmetrical sectoral pattern.

To more demonstrate the validity of Fourier method, a relatively complex case, a sector beam pattern design, is attempted here. In this design, the same 16-element array in Fig. 1 is used, but both excitation magnitudes and phases of the array elements are to be optimized to shape the antenna pattern [7]. This offers 16 columns for magnitudes and 16 columns for phases, is adopted in this sector beam pattern synthesis.

In Figs. 5, 6 and 7, three design examples having sector beam:

$[\varphi_1,\varphi_2]=[50^\circ, 120^\circ]$, or center $\varphi_c = 85^\circ$ and width $\varphi_b = 30^\circ$.
$[\varphi_1,\varphi_2]=[60^\circ, 100^\circ]$, or center $\varphi_c = 80^\circ$ and width $\varphi_b = 40^\circ$.
$[\varphi_1,\varphi_2]=[75^\circ, 80^\circ]$, or center $\varphi_c = 77.5^\circ$ and width $\varphi_b = 5^\circ$.

The number of array elements was N = 16, with half-wavelength spacing d = $\lambda/2$. The stopband attenuations A = 30dB. The desires for the sector beam pattern are shown in Fig 5 using dashed lines. To define the sector beam, there are two specific angular regions. Region I ranges from 50° to 120°, Region II controls the sidelobe levels, which are all below 30 dB and between (135° and 180°) and (0° and 30°).

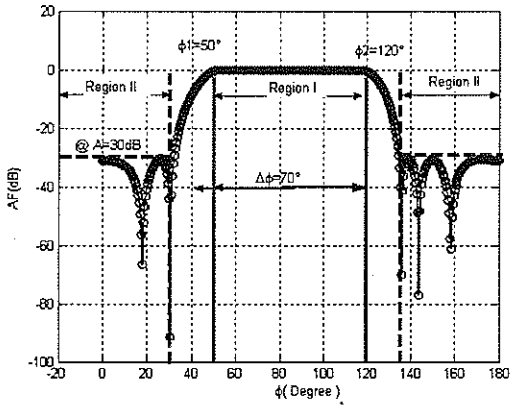

Figure 5 : Sector Beam Pattern Of An 16-element Linear Array. The Dashed Lines Are The Desired Pattern, Which Requires Ripples In Region I at [50° ;120°] And Sidelobe Levels In Region Ii Lower Than -30 dB.

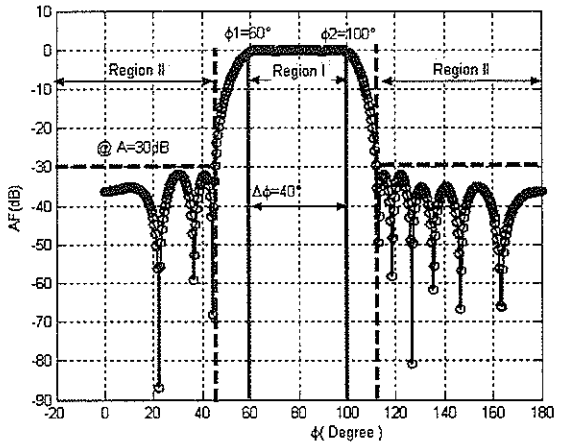

Figure 6 : Sector Beam Pattern Of An 16-element Linear Array. The Dashed Lines Are The Desired Pattern, Which Requires Ripples In Region I At [60°; 100°] And Sidelobe Levels In Region Ii Lower Than -30 Db.

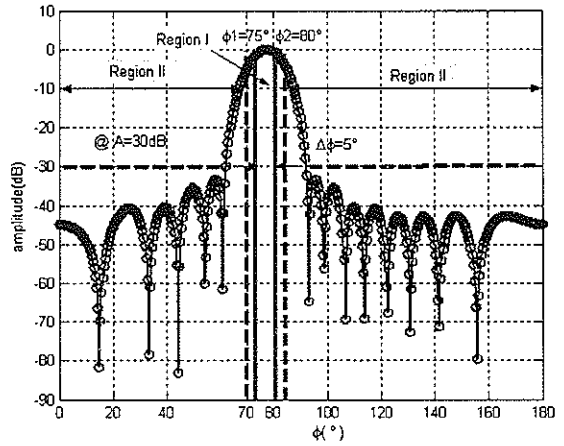

Figure 7 : Sector Beam Pattern Of An 16-Element Linear Array. The Dashed Lines Are The Desired Pattern, Which Requires Ripples In Region I At [75° ; 80°]And Sidelobe Levels In Region Ii Lower Than -30 Db.

TABLE 1

Computed Element Phases and Magnitude for Figures 5,6 And 7

	Synthesized excitations					
	$\varphi_1 = 50^\circ$ $\varphi_2 = 120^\circ$		$\varphi_1 = 60^\circ$ $\varphi_2 = 100^\circ$		$\varphi_1 = 75^\circ$ $\varphi_2 = 80^\circ$	
	$\Delta\varphi = 70^\circ$		$\Delta\varphi = 40^\circ$		$\Delta\varphi = 5^\circ$	
	Fig.5		Fig.6		Fig.7	
A	30dB		30dB		30dB	
m	$\arg i(m)$	$\lvert i(m)\rvert$	$\arg i(m)$	$\lvert i(m)\rvert$	$\arg i(m)$	$\lvert i(m)\rvert$
1	-83.61	0.0029	40.28	0.0137	111.9154	0.0046
2	83.53	0.0235	-169.08	0.0112	-107.0067	0.0046
3	-109.32	0.0290	161.54	0.0350	-145.9287	0.0216
4	-122.17	0.0052	-47.82	0.0038	175.1492	0.0459
5	44.97	0.0674	-77.19	0.0742	136.2272	0.0747
6	-147.87	0.0956	-106.57	0.0346	97.3051	0.1037
7	-160.72	0.0068	44.05	0.1777	58.3831	0.1277
8	6.42	0.5483	14.68	0.4004	19.4610	0.1420
9	-6.42	0.5483	-14.68	0.4004	-19.4610	0.1420
10	160.72	0.0068	-44.05	0.1777	-58.3831	0.1277
11	147.87	0.0956	106.57	0.0346	-97.3051	0.1037
12	-44.97	0.0674	77.19	0.0742	-136.2272	0.0747
13	122.17	0.0052	47.82	0.0038	-175.1492	0.0459
14	109.32	0.0290	-161.54	0.0350	145.9287	0.0216
15	-83.53	0.0235	169.08	0.0112	107.0067	0.0046
16	83.6184	0.0029	-40.28	0.0137	-111.9154	0.0046

Table 1 illustrates the wave number translation process and the corresponding rotation of the angular pattern, for an 16-element uniform array with d = $\lambda/2$, steered for different sectors [50°, 120°], [60°, 100°] and [75°, 80°].

Figs 8, 9 and 10 shows the synthesized radiation pattern of 16-element multibeam arrays with half wavelength spacing, and steered towards the different angles @45°, @90°, @120° and @150°. The broadside array was designed as a Taylor-Kaiser array with sidelobe level of R = 50, R=40 and R = 30 dB.

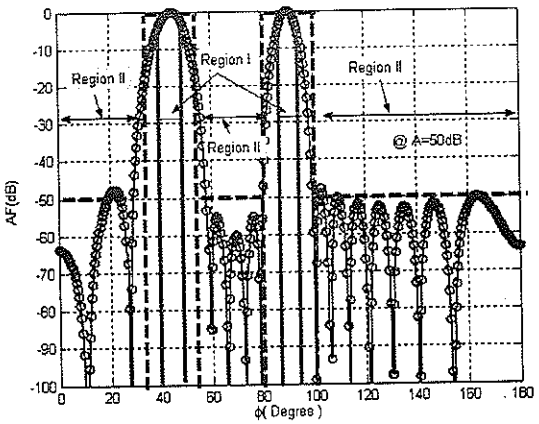

Figure 8 : Multibeam Arrays (2 beams @45° and @90°) s with A = 50 dB Sidelobes.

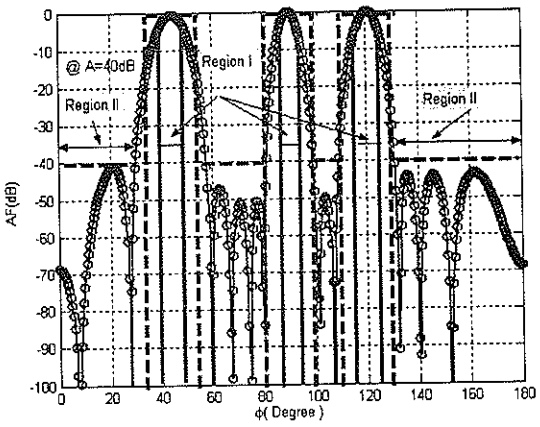

Figure 9 : Multibeam arrays (3 beams@45°, @90° and @120°) with A = 40 dB Sidelobes.

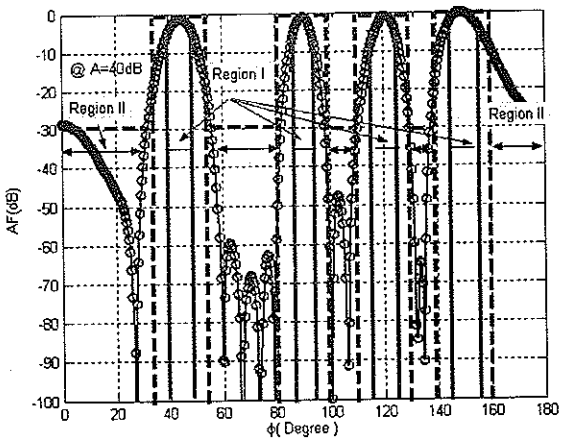

Figure 10 : Multi-beam Arrays (4 beams @50°, @90°, @120° and @150°) with A = 30 dB Sidelobes.

Table 2 illustrates the wavenumber translation and the corresponding rotation of multibeam antenna array for 16 elements uniform array with d = ?/2, steered for different angles (2 beams @45 o and 90o) with sidelobe level A=50dB, (3 beams @45 o,90 o and 120 o) with A=40dB and (4 beams @50 o,90 o,120 o and 150 o) with A=30dB

Table : 2 Computed Element Phases And Magnitude For Fiures 8,9 And 10

	Synthesized excitations					
	$\varphi_1 = 50^o$ $\varphi_2 = 120^o$		$\varphi_1 = 60^o$ $\varphi_2 = 100^o$		$\varphi_1 = 75^o$ $\varphi_2 = 80^o$	
	$\Delta\varphi = 70^o$		$\Delta\varphi = 40^o$		$\Delta\varphi = 5^o$	
	Fig.5		Fig.6		Fig.7	
A	30dB		30dB		30dB	
m	$\arg i(m)$	$\lvert i(m)\rvert$	$\arg i(m)$	$\lvert i(m)\rvert$	$\arg i(m)$	$\lvert i(m)\rvert$
1	-83.61	0.0029	40.28	0.0137	111.9154	0.0046
2	83.53	0.0235	-169.08	0.0112	-107.0067	0.0046
3	-109.32	0.0290	161.54	0.0350	-145.9287	0.0216
4	-122.17	0.0052	-47.82	0.0038	175.1492	0.0459
5	44.97	0.0674	-77.19	0.0742	136.2272	0.0747
6	-147.87	0.0956	-106.57	0.0346	97.3051	0.1037
7	-160.72	0.0068	44.05	0.1777	58.3831	0.1277
8	6.42	0.5483	14.68	0.4004	19.4610	0.1420
9	-6.42	0.5483	-14.68	0.4004	-19.4610	0.1420
10	160.72	0.0068	-44.05	0.1777	-58.3831	0.1277
11	147.87	0.0956	106.57	0.0346	-97.3051	0.1037
12	-44.97	0.0674	77.19	0.0742	-136.2272	0.0747
13	122.17	0.0052	47.82	0.0038	-175.1492	0.0459
14	109.32	0.0290	-161.54	0.0350	145.9287	0.0216
15	-83.53	0.0235	169.08	0.0112	107.0067	0.0046
16	83.6184	0.0029	-40.28	0.0137	-111.9154	0.0046

4. Synthesis Using Neural Networks

The NNs (Neural Networks) have to be trained with as set of the input-output data pairs. The radiation pattern is used as the input data, and the design parameters (i_m, φ_m) are used as the output data. The array factor can be sample at different angles and presented to the NN. Regardless of the NN architecture chosen to solve this problem, to describe the pattern correctly, a large numbers of samples are necessary, and the number varies with the complexity of the pattern.

All input data presented to the NNs [8] have to be normalized so their range varies from 0 to 1. The array factor is normalized next. The element distances are expressed in terms of wavelengths and their excitation is normalized with the magnitude of the largest excitation of the elements of that particular array.

To check if the network can predict the excitations (amplitude and phase) required, a training file is created with the Fourier coefficients of the array factor as the input and the number of elements, expressed in binary format as the output.

An MLP, with back-propagation algorithm training was used with matlab 6.5 toolbox. The NNs consisted 17 input nodes, $\lfloor x_1(p),..., x_{17}(p) \rfloor$ and 16 output nodes (16 antenna array), and one hidden layer.

A neural network is a considerable and parallel computation structure composed by nonlinear individual units known as neurons. The knowledge contained in the network is obtained through a learning process and is stored at the interconnections between neurons. A simplified model for a neuron is shown in Fig. 11. Its behavior is expressed as:

$$y = \varphi\left(\sum_{j=1}^{P} w_j x_j - \theta\right) \qquad (23)$$

Where

$\varphi(\cdot)$ is the activation function, are the weights applied to each input x_k, $k = 1,..., K$ are the inputs, and θ is the threshold or bias term. This simplified model is known as perceptron. The activation function allows separation of inputs through hyperplanes. The most common activation function is sigmoid.

The process to train and test a designed neural network:

1) We make training patterns and test patterns.

2) The neural network architecture is designed and trained by newff MATLAB function with input patterns and training parameters.

3) We can easily check the result by using a sim MATLAB function.

Training Patterns (input data)

Input (x): $\lfloor x_1,...,x_{17} \rfloor$ (17 Sector beam) with $x_k \in [0,1]$

Desired output : $\lfloor i_{d1}\angle\varphi_{d1}$,..., $i_{d16}\angle\varphi_{d16} \rfloor$ (Desired amplitude and phase synthesized by Fourier transform method)

Table : 3 Typical Values Of Parameters Use In Back-propagation Algorithm

Parameters	Symbol	value
Neuron in the input layer	K	17
Neuron in the output layer	I	16
Neuron in the hidden layer	J	30
coefficent of training	η	0.03

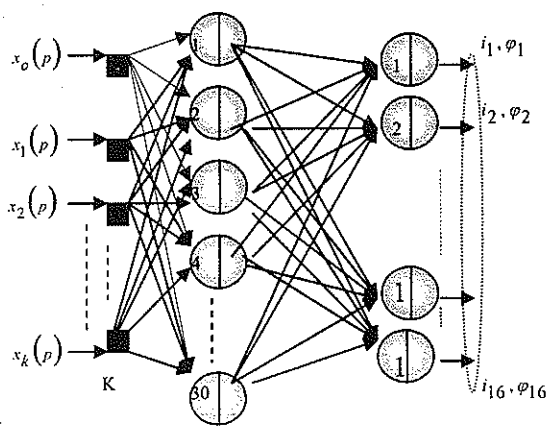

Figure 11 : The Neural Beamformer Architecture

Fig.11 shows the architecture of network after training:

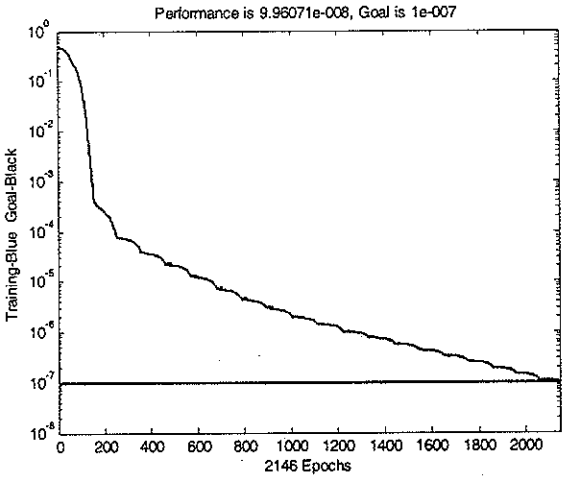

Figure 12 : Performance

The training phase is illustrated in Fig.12. It represents the evolution of the mean square error between exits of the NN and samples given according to the number of epochs, the gotten final error is $9.96071\ 10^{-8}$.

5. Simulation And Measurement Result

The proposed scheme has been tested with good results. An 8 element collinear half-wavelength (band 2 to 2.7 GHz) quasi-yagi array with centers separated is now used for synthesis purposes considering voltages with variable amplitude and phase.

The geometry of the quasi-yagi array and its feeding system with all the geometrical parameters is shown in Fig.13. The final dimensions of the circuit are:

$W_1 = W_3 = W_4 = W_5 = W_{Dir} = 3.16$ mm;

$W6 = S = 1.58$ mm;

$W_{Dip} = 4$ mm;

$S_{Ref} = 25$ mm; $S_{Dri} = S_{Dir} = 19$ mm;

$L_{Dri} = 54$ mm; $L_{Dri} = 24$ mm ; $L_{Ref} = 65$ mm.

These dimensions have been obtained after optimisation of the total circuit. As the microstrip to coplanar stripline

transition exhibits good characteristics, only the antenna geometry and the coplanar stripline dimensions have been adjusted manually. The following sub-sections reports the characteristics of the optimum antenna in terms of input impedance response and radiation characteristics.

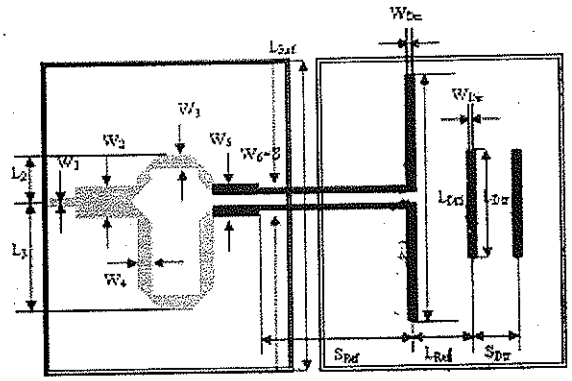

Figure 13 : Geometry Of The Quasi-yagi Antenna

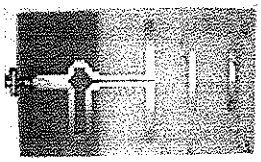

Figure 14 : Antenna(quasi-Yagi)

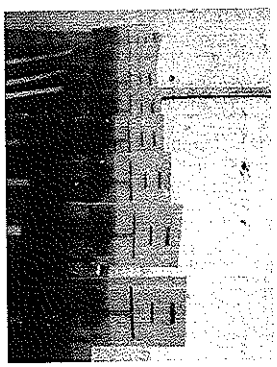

Figure 15 : 8-Element Prototype

The optimized antenna was first simulated on an infinite substrate with the Advanced Design system 2002. The results of the reflection coefficient from both simulations and measurement [12] are compared in Fig 16.

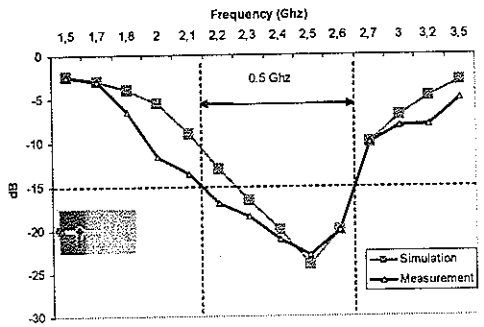

Figure 16 : Measured and Simulated S_n

Fig.16 shows the simulation and measurement results for the antenna (quasi-Yagi) at the resonant frequency.

The characteristics of the antenna were simulated between 1.4 GHz and 3.6 GHz. Fig 17 and Fig.18 present the profit of the antenna according to the frequency.

In short, the antenna with the following characteristics:

- Band-width: 450 MHz centred to 2.45 GHz.
- Gain: 7.743 dB.
- Directivity: 15.484.
- The -3dB width: 125 degrees in the plan H and 80 degrees in the plan E.

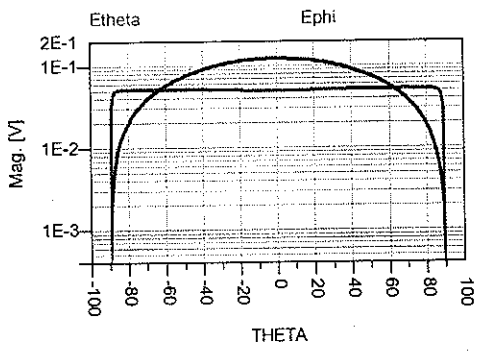

Figure 17 : Radiation Pattern In The Plan E (φ=90°) And In The Plan H (φ=0°) (Elementary Antenna)

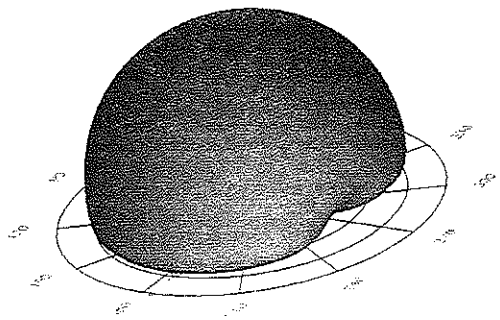

Figure 18 : Radiation Pattern (E phi) (f=2.4583 GHz, Elementary antenna)

A- Prototype

A prototype of 8 collinear half-wavelength slots with as separation between consecutive slot centers has been designed and constructed for a frequency 2 to 2.7 GHz. The antenna has been constructed using a feeding network based on microstrip transmission lines with feeding values (attenuation and phase shift) calculated using the proposed Wilkinson techniques. The feeding network is shown in Fig. 19. In our study one will replace this technology by a neural networks model.

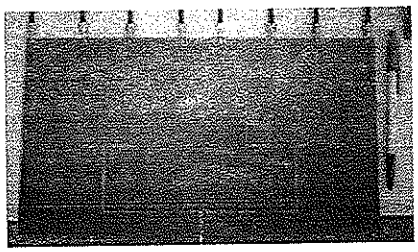

Figure 19. Feeding Network Of The Prototype.

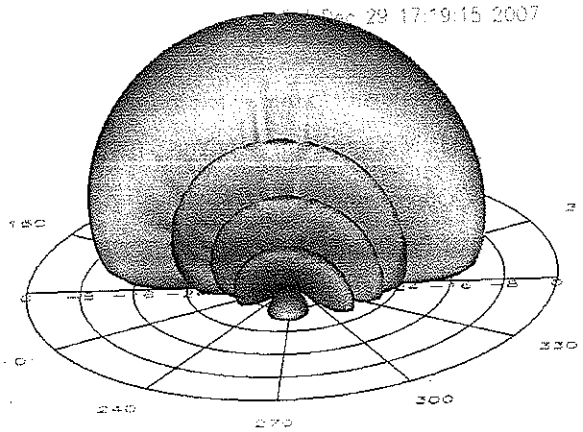

Figure. 20. Radiation Pattern (f=2.45 GHz, 8-Element antenna quasi-yagi) In Plan 1

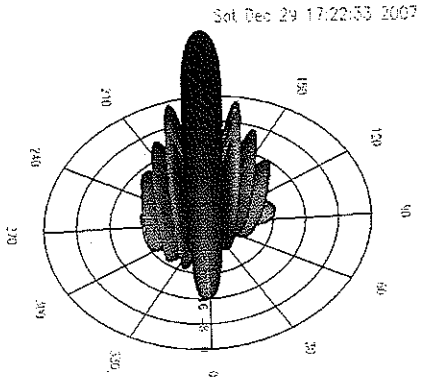

Figure 21. Radiation Pattern (f=2.45 GHz, 8-Element antenna quasi-yagi) In Plan 2

Fig.20 and Fig.21 present the radiation pattern simulated with Advanced Design system 2002 in two different angles from visualizations with a uniform excitation, therefore the form of the radiation obtained on the desired frequency band.

The profit is indeed with its maximum for angles close to 0° and the diagram present moreover one quasi-perfect symmetry.

B-switched Beam Smart Antenna System

A switched beam smart antenna system can be realized by breaking the whole system down into four major building blocks for ease of analysis [9].

The switched-beam arrays comprise beamforming networks and a beam selection neural model, as shown in Fig.20.

The neural model selects the beam with maximum power response by switching the beams. However, the adaptive array antennas incorporate more intelligence than the switched beam arrays.

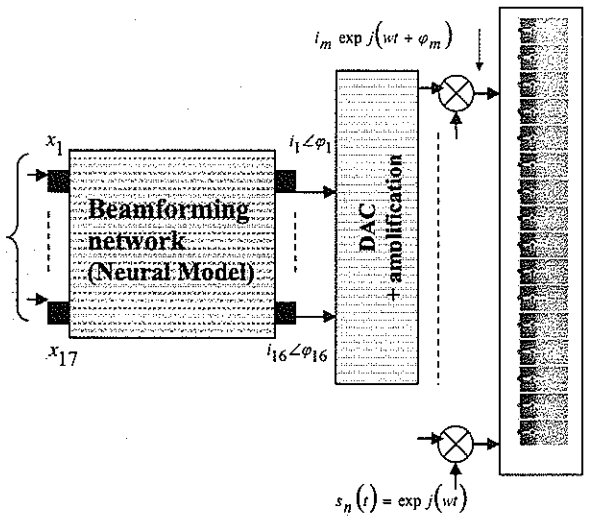

Figure : 22 Schematic Diagram Of A Beamforming Network

The Neural networks are a suitable beamforming network that can be used together with an antenna array for switched beamforming. Sector beam and multibeam are formed and steered towards the desired user to minimize interference from other users, using less transmit power as compared to an omni-directional antenna. There has to be a phase change at each of the radiating antenna element so that the wavefront formed will give a number beams.

This switched beam system works based on the strength of power and a neural model [10-11]. The implementation incorporates the use of a linear antenna fed by neural network as a beamforming network, with possible method of improving DOA resolution being incorporated.

6. Conclusion

In this paper, a global optimization technique based on Fourier transform method and neural network technique are applied so as to determine the excitation coefficients and the resultant pattern for a broadside discrete element array whose array factor will directly approximate the symmetrical sectoral pattern.

The implementation system is described in detail, and linear antenna array examples are discussed to demonstrate its validity. Optimized results show that the desired array factors, a null controlled pattern and a sector beam pattern, are effectively obtained. It is found that neural network is an excellent candidate for optimizing diverse applications, as it is easy to realize and converges to the desired patterns rapidly.

Acknowledgment

The authors extend their appreciation to the antonymous reviewers for their valuable comments that contributed to enhance the quality of the presentation of this work. This work was supported by the Lebanese University research project.

References

[I] C. A. Balanis, *"Antenna Theory Analysis and Design"*, John W3ey & Sons, Inc. 1982.

[2] C. Chistodoulou, M. Georgiopoulos, *"Applications of Neural Networks in Electromagnetics"*, Artech House Boston London ,ISBN 0-89006-880-1, PP. 315, 2001.

[3] S. J.orfanidi, *" Electromagnetic Waves & Antennas"*, June 21, 2004

[4] J. W. Goodman, *"Introduction to Fourier Optics"*, 2nd ed., McGraw-Hill, New York, 1996.

[5] A. V. Oppenheim and R. W. Schafer, *"Discrete Time Signal Processing"*, Prentice Hall, Upper Saddle River, NJ, 1989.

[6] E. C. Dufort, *"Pattern synthesis based on adaptive array theory"*, IEEE Trans. Antennas Propagat., Vol. 37, PP. 1011-1018, Aug. 1989.

[7] D. Gies and Y. Rahmat-Samii, *"Particle swarm optimization for recon-figurable phased-differentiated array design"*, Microw. Opt. Technol. Lett., Vol. 38, No. 3, PP. 168-175, Aug. 2003.

[8] D.L.Phillips *"A Technique for the Numerical Solution of Certain Integral Equations of the First Kind"*, Journal of the Association for Computing Machinery, No.9 , PP. 84-97,1962.

[9] Varlamos, P.K. and C. N. Capsalis, *"Electronic beam steering using switched parasitic smart antenna arrays"*, Progress In Electromagnetics Research, PIER 36, 101-119, 2002.

[10] C. A. Olen and R. T. Compton, Jr, *"A numerical pattern synthesis algorithm for arrays"*, IEEE Trans. Antennas Propagat., Vol. 38, PP. 1666-1676, Oct. 1990.

[11] F. Capolino, S. Maci and L. B. Felsen, *"Green's function for a planar phased sectoral array of dipoles"*, Radio Science, Vol. 35, No. 2, PP.579-593, Mar.-Apr. 2000.

[11] F. Capolino, S. Maci and L. B. Felsen, *"Green's function for a planar phased sectoral array of dipoles"*, Radio Science, Vol. 35, No. 2, PP. 579-593, Mar.-Apr. 2000.

[12] V.V.Yem, *"Conception et réalisation d'un sondeur de canal multi-capteur utilisant les corrélateurs cinq-ports pour la mesure de propagation à l'intérieur des bâtiments"*, Dec.2005

Author's Biography

Ridha Ghayoula *received the degree in automatic electric engineering in 2002 and the M.Sc. degrees in electronics device from El-manar University - Sciences' faculty of Tunis, Tunisia, in 2005. He is currently working toward the Ph.D. degree in electrical engineering at the Sciences' faculty of Tunis. His research interests include smart antennas, neural network applications in antennas, adaptive arrays and microwave integrated circuits.*

Najib Fadlallah *received the degree in Telecommunications engineering from the University of Montreal-POLYTECHNIQUE - Canada in 1997 and M. Sc. of High Frequency Electronics & Optoelectronics in 2002 and the Ph.D. degree in 2005 from Limoges University - France. Since 2005, he was with the Department of GRIT at the Lebanese university (Institute of Technology). His current research interests include antennas, array signal processing, smart antennas, and neural network synthesis beamforming model for adaptive antenna arrays.*

Ali Gharsallah *received the degree in radio-electrical engineering from the Ecole Supérieure de Télécommunication de Tunis in 1986 and the Ph.D. degree in 1994 from the Ecole Nationale d'Ingénieurs de Tunis. Since 1991, he was with the Department of Physics at the Faculty of Sciences, Tunis. His current research interests include antennas, array signal processing, multilayered structures and microwave integrated circuits.*

Mohamed Rammal *received the degree in Telecommunications engineering from the Lebanese University- Beyrouth in 1988 and M. Sc. of High Frequency Electronics & Optoelectronics in 1990 and the Ph.D. degree in 1993 from Limoges University - France. Since 2005, he was with the Department of GRIT at the Lebanese university (Institute of Technology). His current research interests include antenna arrays synthesis, smart antennas, and neural network Synthesis beamforming model for adaptive antenna arrays.*